J|A|C|S
ARTICLES

Published on Web 08/05/2009

Molecular Simulation of Electric Double-Layer Capacitors Based on Carbon Nanotube Forests

Lu Yang,[†,§] Brian H. Fishbine,[†] Albert Migliori,[†] and Lawrence R. Pratt*[,‡]

Los Alamos National Laboratory, Los Alamos, New Mexico, New Mexico 87545, and Department of Chemical and Biomolecular Engineering, Tulane University, New Orleans, Louisiana 70118

Received June 2, 2009; E-mail: lpratt@tulane.edu

Abstract: Described here are the first simulations of electric double-layer capacitors based on carbon nanotube forests modeled fully at a molecular level. The computations determine single-electrode capacitances in the neighborhood of 80 F/g, in agreement with experimental capacitances of electric double-layer capacitors utilizing carbon nanotube forests or carbide-derived carbons as electrode material. The capacitance increases modestly with the decrease of the pore size through radii greater than 1 nm, which is consistent with recent experiments on carbide-derived carbon electrodes. Because the various factors included in these simulations are precisely defined, these simulation data will help to disentangle distinct physical chemical factors that contribute to the performance of these materials, *e.g.*, pore geometry, variable filling of the pores, pseudocapacitance, and electronic characteristics of the nanotubes.

Depletion of fossil fuels, increased energy consumption, and the desirability of low CO_2 emissions have heightened the need for efficient, clean, and renewable energy sources.[1] Many carbon-neutral renewable energy resources, e.g. solar and wind, are intermittent and require effective energy storage. Efficient, high energy-density electrical energy storage systems would also play a role in design of electric vehicles and would facilitate effective power supply from the grid. Here we present the first molecular-scale calculations on the performance of electrochemical capacitors based on carbon nanotube (CNT) forests as electrodes, systems proposed to respond to these needs.

Recently proposed electric double-layer capacitors (EDLCs) with electrodes of aligned, single-wall (SW) CNTs can have capacitances exceeding those of conventional EDLCs.[2−4] Nanotube-based EDLCs offer possibilities for deliberate nanoscale mechanical and chemical design and for switching times possibly faster than those found with activated carbon. The natural goal for such capacitors would be to achieve energy densities comparable to those of current battery systems, but also to retain the traditional advantages of capacitors, namely faster response (thus advantageous power densities) and longer cycle lifetimes.

Carbon nanotubes can be chemically stable and can have higher conductivities than activated carbon.[5] Higher conductivity reduces switching times and resistive losses. Despite the progress in the synthesis of carbon nanotube forests (CNFs), several basic physical chemistry issues associated with their function and the role of the solution have not been characterized at a molecular level that would be relevant to the design of these systems. Examples include the effect of pore size on solution access and on the capacitance, the role of the electrolyte, and molecular time-scale dynamical processes that establish the fastest responses.

Molecular simulations are well suited to address the above issues. We have performed all atom simulations of experimental systems containing oriented parallel metallic CNTs under periodic boundary conditions. Figure 1 illustrates the system treated and gives technical parameters of the setup. Figure 2 gives a molecular depiction of the solution structure for the narrowest-case pore (radius $R = 1.17$ nm) studied here, case 8 of the cases detailed in Table 1. For several of those cases, Figure 3 shows the radial distributions of N/TEA^+ and B/BF_4^- atoms from the center of a charged CNT. As expected, the TEA^+ ions absorb strongly at the surface of the negatively charged CNT, and then many BF_4^- ions are located just outside that inner shell due to attractive electrostatic interactions (upper panel). This whole distribution of charge provides the polarization that is the basis of the double-layer capacitance. In the present case, the innermost shell of ions has a regional concentration that is 47 times higher than the bulk concentration. With a positively charged CNT, the maximum radial density due to the innermost BF_4^- ions was about 25 times the bulk density, a slightly weaker absorption than for the positive ions to the negatively charged CNT. This is due to the stronger solvation of the smaller BF_4^- ions, and perhaps also to some intrinsic solvophobicity of TEA^+ ions. The inset of Figure 3

[†] Los Alamos National Laboratory.
[‡] Tulane University.
[§] Current address: Applied Materials, Santa Clara, CA 95052.

(1) Basic research needs for electrical energy storage, Report of the Basic Energy Sciences Workshop for Electrical Energy Storage; Office of Basic Energy Sciences, Department of Energy: Washington, DC, 2007; www.science.doe.gov/bes/reports/files/EES_rpt.pdf.
(2) Futaba, D. N.; Hata, K.; Namai, T.; Yamada, T.; Mizuno, K.; Hayamizu, Y.; Yumura, M.; Iijima, S. *J. Phys. Chem. B* **2006**, *110*, 8035–8038.
(3) Futaba, D. N.; Hata, K.; Yamada, T.; Hiraoka, T.; Hayamizu, Y.; Kakudate, Y.; Tanaike, O.; Hatori, H.; Yumura, M.; Iijima, S. *Nat. Mater.* **2006**, *5*, 987–994.
(4) Hata, K.; Futaba, D. N.; Mizuno, K.; Namai, T.; Yumura, M.; Iijima, S. *Science* **2004**, *306*, 1362–1364.
(5) Flahaut, E.; Peigney, A.; Laurent, C.; Marliere, C.; Chastel, F.; Rousset, A. *Acta Mater.* **2000**, *48*, 3803–3812.

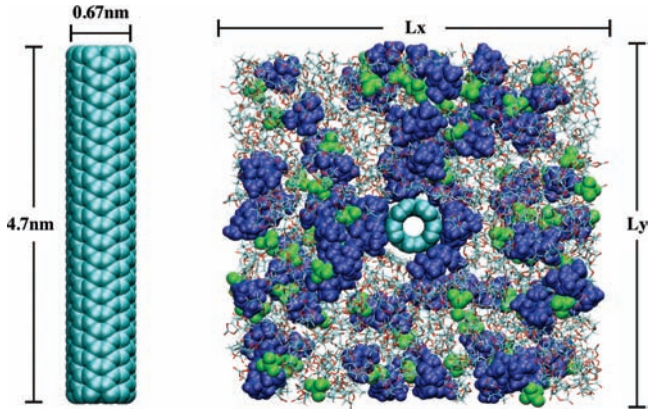

Figure 1. Illustration of the filled nanotube forest treated by simulation with periodic boundary conditions. (Left) The nanotube model. (Right) Cross-section perpendicular to the nanotubes. This configuration resulted after 30 ns of the thermal motion from an initial configuration in which the solution structure was approximately uniform. We used a piece of (5,5) armchair CNT comprising 390 carbons with a C−C tube diameter of 0.67 nm and length of 4.7 nm. A total charge of $Q = ne$, with n and other simulation details listed in Table 1, was distributed uniformly among the 390 CNT atoms so that each atom carried a charge of ne/390, to mimic the charged/discharged behavior of the capacitor. These charged conditions represent a charge density ranging from −0.23 to 0.23 C/m^2. Partial charges are assigned to atomic sites of tetraethylammonium (TEA^+) and tetrafluoroborate (BF_4^-) ions according to the recommendations of Luzhkov et al.[6] and Andrade et al.,[7] respectively. All the other parameters are taken from general AMBER force field (GAFF).[8] Shown here is case 1 using $L_x \approx L_y \approx 6$ nm, 1000 propylene carbonate molecules. The numbers of BF_4^- or TEA^+ ions were adjusted to constitute a neutral system including the charge n on CNT. We typically sought bulk electrolyte concentrations in the middle of the pores (the space between the tubes) near 1.0 M.[9] Table 1 gives specific ion/molecule numbers; note that cases 7 and 8 correspond to significantly higher concentrations. To investigate the effect of pore size, we simulated smaller systems, with shorter CNT−CNT distances, containing therefore less propylene carbonate and fewer $TEA^+BF_4^-$ ions, as listed in Table 1. Trajectories were constructed with a time step of 2 fs, using the isothermal−isobaric (NPT) ensemble with the Langevin thermostat. Temperature and pressure were 300 K and 1 atm. The simulations were performed with AMBER9.[10] Electrostatic interactions were calculated using particle mesh Ewald with a grid spacing of 1 Å. All simulations lasted 30 ns, with the first 10 ns discarded as aging. We confirmed that this equilibration was satisfactory by extending one calculation (case 3) for another 5 ns using parallel tempering utilizing temperatures of 300, 325, 345, and 360 K. Study of systems with the same electrolyte concentration and CNT charge density but with a CNT length of 9.6 nm confirmed that the present results do not depend on CNT length. Separate calculations on homogeneous liquid propylene carbonate verified that this model gives an accurate value for the linear response dielectric constant and its temperature dependence.[11]

shows the radial distribution of N/TEA^+ and B/BF_4^- atoms from the center of the discharged CNT and confirms this interpretation. When the CNT was discharged, we still observed the principal TEA^+ peak next to the CNT surface with the density 2.3 times higher than bulk density. Favorable electrostatic interactions with this initial TEA^+ layer then serve to position the first BF_4^- layer. The solvent (PC) molecules were not excluded from the inner double region of the charged CNTs, but the structuring of their radial distribution (not shown) was not as pronounced as for the ions.

The capacitance C measured for a typical two-electrode system is

$$\frac{1}{C} = \frac{1}{C_+} + \frac{1}{C_-} \qquad (1)$$

where C_+ and C_- are the capacitances of positively and negatively charged electrodes, respectively. We evaluate the double-layer capacitance of a single electrode by setting the net charge on the surface of the electrode and determining the electrostatic potential at the electrode surface, ϕ(surface), relative to the electrostatic potential in the electrolyte solution. This difference is obtained from

$$\Delta\phi(r) \equiv \left(\frac{-1}{2\pi\varepsilon_0}\right)\int_0^r Q(\lambda)\frac{d\lambda}{\lambda} = \phi(r) - \phi(\text{surface}) \qquad (2)$$

integrating Poisson's equation assuming cylindrical geometry. $Q(\lambda)$ is the total charge enclosed in a cylinder of radius λ parallel to the nanotube and centered on it. Specifically, when $\Delta\phi$ plateaus for large r, this is the electrostatic potential deep in

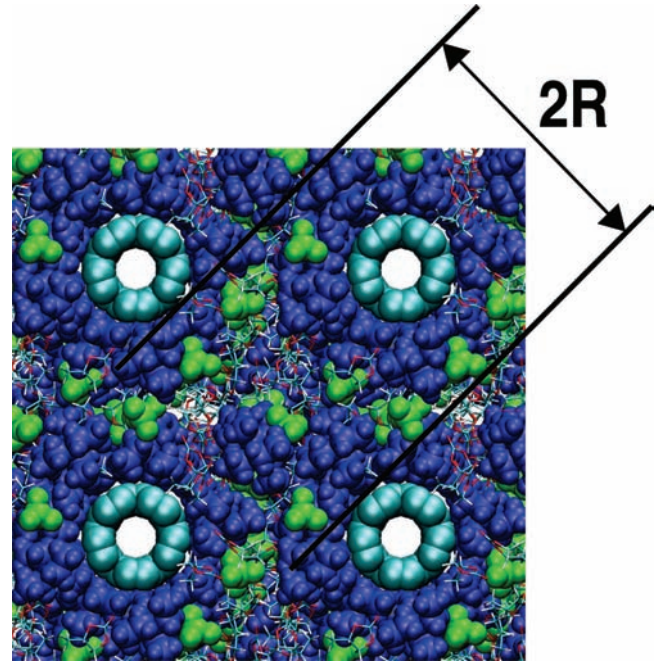

Figure 2. Snapshot of the electrical double layer formed around the negatively charged CNT with charge density of −0.23 C/m^2 and $R = 1.17$ nm. Cross-section of the simulation cell perpendicular to the nanotubes (four images are shown). The blue balls depict the tetraethylammonium (TEA^+) ions, the green balls represent the tetrafluoroborate (BF^-) ions, and the stick figures show the propylene carbonate molecules. This suggests an inner-shell structure dominated by TEA^+ cations to the exclusion of BF_4^- anions when the CNT is negatively charged.

Table 1. Collected Parameters and Results of the Calculations[a]

calculation	R (nm)	Q/e	$\Delta\phi$ (V)	N_{TEA^+}	$N_{BF_4^-}$	N_{PC}	C (μF/cm^2)
case 1	3.94	−14	4.09	85	71	1000	5.53
case 2	2.59	−14	3.97	43	29	500	5.72
case 3	1.85	−14	4.00	21	7	250	5.66
case 4	2.70	14	−3.53	29	43	500	6.42
case 5	1.85	−10	2.83	21	11	250	5.72
case 6	1.85	−5	1.47	21	16	250	5.50
case 7	1.37	−14	3.80	43	29	100	5.97
case 8	1.17	−14	3.73	21	7	100	6.08
case 9	2.59	0		43	43	500	

[a] R, taken as the pore radius, is half the next-nearest-neighbor CNT surface-to-surface distance, see Figure 2. The electrostatic potential of the uncharged case was approximately −0.07 V, a negligible magnitude in these considerations.

(6) Luzhkov, V. B.; Osterberg, F.; Acharya, P.; Chattopadhyaya, J.; Aqvist, J. *Phys. Chem. Chem. Phys.* **2002**, *4*, 4640–4647.
(7) de Andrade, J.; Boes, E. S.; Stassen, H. *J. Phys. Chem. B* **2002**, *106*, 13344–13351.
(8) Wang, J. M.; Wolf, R. M.; Caldwell, J. W.; Kollman, P. A.; Case, D. A. *J. Comput. Chem.* **2004**, *25*, 1157–74.

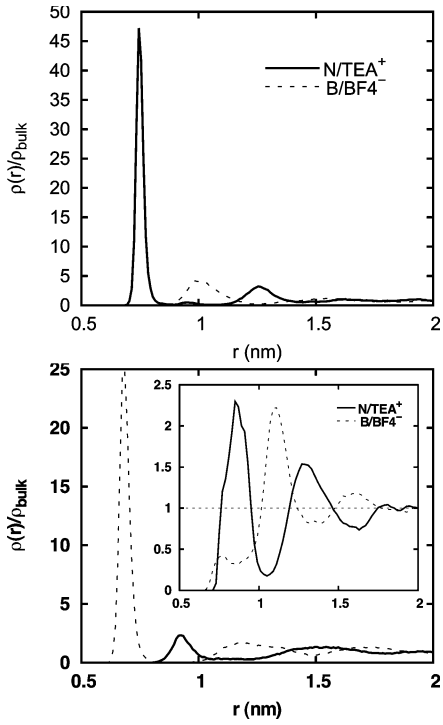

Figure 3. Local number density of N/TEA^+ and B/BF_4^- ions radially from the center of the charged CNTs, with surface charge density of -0.23 C/m^2, $R = 2.59$ nm (upper panel, case 2 of Table 1) and surface charge density of 0.23 C/m^2, $R = 2.70$ nm (lower panel, case 4 of Table 1). The inset shows results for case 9 of Table 1, for which the CNT is uncharged.

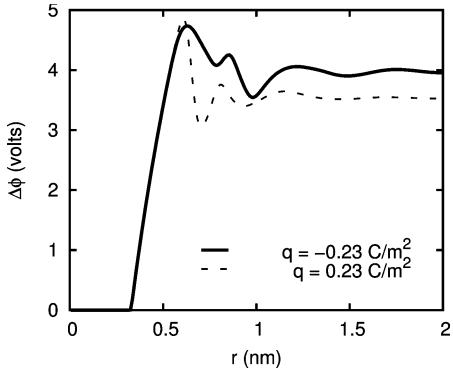

Figure 4. (Solid line) For system with surface charge density of -0.23 C/m^2, $R = 2.59$ nm (case 2), the average electrostatic potential in the solution obtained using eq 2. (Dashed line) $-\Delta\phi$ for a system with surface charge density of 0.23 C/m^2, $R = 2.70$ nm (case 4).

the electrolyte phase relative to the nanotube; thus, $\Delta\phi$ is positive for a negatively charged nanotube. Figure 4 shows how the observed electrostatic potentials depend on r; the electrostatic potential differences saturate in radial distances of about 1 nm from the CNT surface. The single-electrode capacitances are the amount of charge on the CNT divided by the potential difference between the CNT and the bulk electrolyte. Table 1

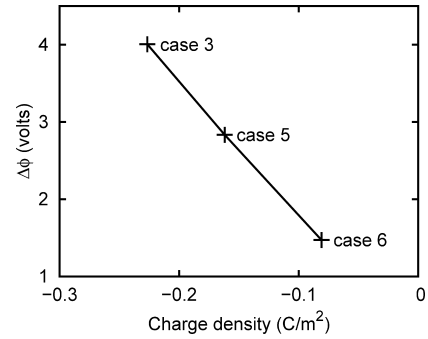

Figure 5. Electrostatic potential difference as a function of charge density on the CNT surface. Here $R = 1.85$ nm.

gives the electrostatic potential differences for both negatively and positively charged CNTs. For example, for cases 2 and 4 of Table 1, the charge density on the CNT is -0.23 and 0.23 C/m^2, and the net electrostatic potential change is approximately 4 and 3.5 V, resulting in specific capacitances of 5.7 and 6.4 μF/cm^2, respectively. If we assume that 1300 m^2/g is the specific surface area for these tubes, the specific capacitances are 74 and 83 F/g. These values are in remarkably good agreement with recent measurements[12] of single-electrode capacitances of negatively (71 F/g) and positively (82 F/g) charged SWCNT electrodes with the same electrolyte and acetonitrile solvent. The overall capacitances (eq 1) also agree well with the experimental measurements on CNT forests or carbide-derived carbons as electrode materials.[9,13,14]

As noted, the calculated capacitances are consistent with experiment[15] in the asymmetry between negative and positive electrodes. Although the charge accumulation of BF_4^- ions in response to the positively charged CNT is smaller than that of TEA^+ in response to the negatively charged CNT (as shown in Figure 3), the potential difference is smaller for the positively charged CNT, which means that BF_4^- ions are more effective in balancing the positively charged CNT. The smaller size BF_4^- ions approach the surface of the positively charged CNT more closely, leading to a larger capacitance.[13]

The dependence of $\Delta\phi$ on charge (Figure 5) shows insignificant curvature, so the capacitances inferred here are insensitive to potential for the potential range covered. In contrast, initial experimental measurements[16] for these materials indicate a strong but featureless increase in capacitance with potentials up to 4 V. Improved filling of the pores with increasing electrical potential is one possibility. But recent experiments[17−19] also

(9) Futaba, D. N.; Hata, K.; Yamada, T.; Hiraoka, T.; Hayamizu, Y.; Kakudate, Y.; Tanaike, O.; Hatori, H.; Yumura, M.; Iijima, S. *Nat. Mater.* **2006**, *5*, 987–994.
(10) Case, D. A.; et al. *AMBER 9*; University of California: San Francisco, 2006.
(11) *Dielectric saturation of liquid propylene carbonate in electrical energy storage applications*; Los Alamos National Laboratory Technical Report LA-UR-08-3038; Los Alamos National Laboratory: Los Alamos, NM, 2008.
(12) Ruch, P. W.; Hardwick, L. J.; Hahn, M.; Foelske, A.; Kötz, R.; Wokaun, A. *Carbon* **2009**, *47*, 38–52.
(13) Chmiola, J.; Yushin, G.; Gogotsi, Y.; Portet, C.; Simon, P.; Taberna, P. L. *Science* **2006**, *313*, 1760–1763.
(14) Simon, P.; Gogotsi, Y. *Nat. Mater.* **2008**, *7*, 845.
(15) Chmiola, J.; Largeot, C.; Taberna, P.-L.; Simon, P.; Gogotsi, Y. *Angew. Chem., Int. Ed.* **2008**, *47*, 3392–3395.
(16) Hatori, H.; Tanaike, O.; Imoto, K.; Futaba, D.; Hata, K. Electrochemical Capacitors using Impurity-free Single-walled Carbon Nanotubes. *N4 - Carbon Nanotubes and Nanostructures: Applications and Devices*; Presented at the 209th ECS Meeting, Denver, CO, May 7−12, 2006; The Electrochemical Society: Pennington, NJ, 2006; Abstract 688.
(17) Kimizuka, O.; Tanaike, O.; Yamashita, J.; Hiraoka, T.; Futaba, D.; Hata, K.; Machida, K.; Suematsu, S.; Tamamitsu, K.; Saeki, S. *Carbon* **2008**, *46*, 1999–2001.
(18) Lu, W.; Henry, K. Q. L.; Dai, L. *J. Power Sources* **2009**, *189*, 1270–1277.
(19) Yamada, Y.; Kimizuki, O.; Tanaike, O.; Machida, K.; Suematsu, S.; Tamaitsu, K.; Saeki, S.; Yamada, Y.; Hatori, H. *Electrochem. Solid-State Lett.* **2009**, *12*, K14–K16.

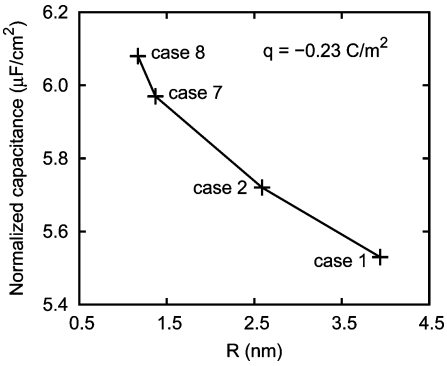

Figure 6. Dependence of the calculated capacitance on pore radius *R*, defined in Figure 2.

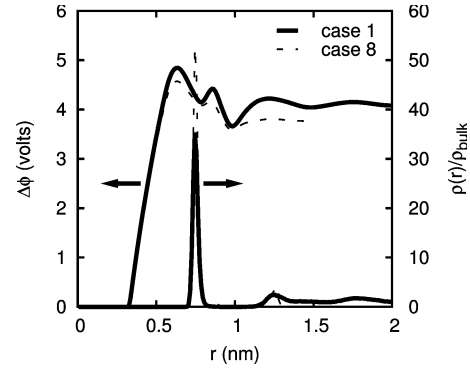

Figure 7. (Lower curves, right axis) Local number density of N/TEA$^+$ radially from the center of the charged CNTs for case 1 ($R = 3.94$ nm) and case 8 ($R = 1.17$ nm). The only difference between the two systems is the radius *R* of the pores. Decreasing the radius of the pores sharpens the spatial variations but does not move them inward appreciably. (Upper curves, left axis) Radial variation of the electrostatic potential relative to the nanotube.

suggest pseudocapacitative behavior and changes in the electronic characteristics of the nanotubes at high potentials. Neither of these issues is addressed by these calculations so far.

Because they are representative, we focus on the negatively charged CNTs to determine how these single-electrode capacitances change with nanotube spacing. Figure 6 shows the specific capacitance as a function of the pore radius. The capacitance increases modestly with the decrease of the pore size through this range of radii, in good agreement with the behavior observed by Chmiola et al.[13] for carbide-derived carbon electrodes in this range of pore sizes. Chmiola et al.[13] also reported an anomalous increase of specific capacitance for even narrower pores.[13,14,20] The geometry of the pores studied here differs from that of the experimental carbide-derived carbon electrodes, and it would be natural to expect some difference in the dependence of capacitance on pore size on that account. Satisfactory extension of the present calculations to narrower pores might require direct simulation of the filling of the pores in deeper systems; i.e., when the cross-sectional area of the pores is smaller, the composition of the pore material is less convincingly estimated but might be addressed on the basis of more aggressive simulation calculations.

Figure 7 indicates how the mean charge density changes with decreasing pore radius *R*. Though the spatial variation sharpens, decreasing *R* does not move the charge distributions inward appreciably. The effect of decreasing *R* is a modest increase of the double-layer capacitance.

Supporting Information Available: Complete ref 10. This material is available free of charge via the Internet at http://pubs.acs.org.

JA9044554

(20) Huang, J.; Sumpter, B. G.; Meunier, V. *Angew. Chem., Int. Ed.* **2008**, *47*, 520–524.